Microstructure and its influence on CH_4 adsorption behavior of deep coal*

Feng Yan-Yan(冯艳艳), Jiang Cheng-Fa(江成发), Liu Dai-Jun(刘代俊)†, and Chu Wei(储 伟)‡

Department of Chemical Engineering, Sichuan University, Chengdu 610065, *China*

(Received 27 March 2013; revised manuscript received 23 May 2013; published online 10 December 2013)

In this paper we investigate the influence of microstructure on the CH_4 adsorption behavior of deep coal. The coal microstructure is characterized by N_2 adsorption at 77 K, scanning electron microscopy (SEM), Raman spectroscopy, and Fourier transform infrared spectroscopy (FT-IR). The CH_4 adsorptions are measured at 298 K at pressures up to 5.0 MPa by the the volumetric method and fitted by the Langmuir model. The results show that the Langmuir model fits well with the experimental data, and there is a positive correlation with surface area, pore volume, I_D/I_G, and CH_4 adsorption capacity. The burial depth also affects the methane adsorption capacity of the samples.

Keywords: CH_4 adsorption, deep coal, pore structure, surface morphology

PACS: 82.80.Dx, 68.43.–h **DOI:** 10.1088/1674-1056/23/2/028201

1. Introduction

At present, the exploitation of methane associated with coal is limited to the under-drainage of mining gas in order to ensure the safety of mining.[1] One of the most important reasons for this outcome is the low permeability of the coal,[2,3] which is an essential factor for coalbed methane (CBM) recovery determined mainly by the coal fracture system.[4–7]

Coal is a polymeric material with a complicated porous structure. There have been many studies focusing on CH_4 adsorption on coal, and considerable research has examined the relationship among CH_4 adsorption capacity, coal characteristics,[8,9] geologic and hydrologic properties.[4,10] The inherent property of coal, which determines the total gas adsorbed under reservoir conditions, and the characteristics of CH_4 adsorption on coal affect CBM migration and recovery.[11] The adsorption capacity of coal is influential. Moreover, the roles played by the location and coal structure are also influential.[6,12–14] The amount of methane which can be physically adsorbed by coals is usually represented as a function of methane pressure, temperature, rank, maceral composition, and moisture content. Apart from those parameters, it is essential to take into account the variations in adsorption capacity of the coals as a function of burial history.

One of the factors controlling methane capacity is the burial depth. Different depths may result in large variations in pore structure,[15] composition, and degree of graphitization. In short, the changing burial depth of the reservoir can result in differences in the adsorption capacity of coal. Thus, CBM exploration should focus on finding the balance between gas extraction and burial depth.[16]

It is important to understand the effect of burial depth on the microstructure of coal.[7,17–19] Currently, there is little work about the effects of microstructural properties on the CH_4 adsorption capacity of coal. Therefore, in this work, we examine the effect of microstructure of coal on CH_4 adsorption behavior. The microstructural properties, including pore structure, degree of graphitization, and composition are used to analyze the variation in the adsorption capacity, from which the adsorption characteristics of deep coals are obtained.

2. Experiment

2.1. Sample preparation

Six bituminous coals, collected at burial depths from 500 m to 1500 m from Datong coal field in Shanxi province (China), were selected as samples. Proximate analysis and ultimate analysis for the coals are given in the following Table 1 and Table 2, respectively. The coal samples were crushed into particles with size fraction of 60–80 mesh. The as-prepared coal particles were dried in an oven overnight at 383 K and stored in sealed plastic containers. The samples were respectively referred to as Coal-1, Coal-2, Coal-3, Coal-4, Coal-5, and Coal-6.

*Project supported by the National Basic Research Program of China (Grant No. 2011CB201202).

†Corresponding author. E-mail: liudj721@163.com

‡Corresponding author. E-mail: chuwei1965scu@163.com

© 2014 Chinese Physical Society and IOP Publishing Ltd

Table 1. Proximate analyses of the samples (air-dried basis, wt%).

Sample	Location	Depth/m	Fixed carbon	Ash	Volatile matter	Moisture
Coal-1	1#	705	58.23	21.21	17.88	2.68
Coal-2	1#	1156	59.90	25.89	11.20	3.01
Coal-3	2#	550	70.35	6.82	19.61	3.22
Coal-4	2#	1362	73.08	13.65	9.59	3.68
Coal-5	3#	601	69.01	8.50	18.98	3.51
Coal-6	3#	978	75.18	7.58	14.19	3.05

Table 2. Ultimate analyses of coal samples.

Sample	C/%	H/%	N/%	S/%	O*/%	O/C ratio
Coal-1	63.42	4.94	< 0.5	< 1.0	30.14	0.475
Coal-2	71.32	5.39	1.79	2.79	18.71	0.262
Coal-3	77.14	5.15	< 0.5	< 1.0	16.21	0.210
Coal-4	82.16	5.34	2.40	3.69	6.41	0.078
Coal-5	80.54	4.42	< 0.5	4.42	10.12	0.126
Coal-6	79.62	5.02	2.48	3.71	9.17	0.115

*calculated by difference.

2.2. Characterization

The textural characterization of coal was based on N_2 adsorption/desorption isotherms, determined at 77 K with a NOVA1000e surface area and pore size analyzer (Quantachrome Company). Samples were degassed at 383 K for 14 h prior to the analysis. The surface area was calculated by the NLDFT method; the micropore (< 10 nm) volume and the pore size distribution were determined by density functional theory (DFT) equation.[15,20]

Surface morphology was investigated by scanning electron microscopy (SEM) (JEOL/EO JSM-5900 microscope).[11,21,22]

The Raman spectrum measurements on coals were conducted with a Raman microspectrometer (Renishaw System InVia) in which an argon laser was used as the excitation source ($\lambda = 514.5$ nm). The spectra were recorded in the wave number range of 400 cm^{-1}–4000 cm^{-1} with a typical exposure time of 2 s.[23,24]

FT-IR analysis of samples was performed on a Nicolet DXC20 FTIR spectrometer.[25–27]

The proximate analysis was investigated by a GF-A6 automatic proximate analyzer (Hebi Celestica Instruments Co, Ltd).[11] The ultimate analysis of samples was performed on a CARLO ERBA 1106 elemental analyzer (Italy). The oxygen content was calculated by difference.

2.3. CH_4 adsorption measurement

The CH_4 adsorption isotherms were measured by the volumetric method by using a gas adsorption apparatus designed by the Northwest Research Institute of Chemical Industry (NWRICI), China.[11] The schematic arrangement is shown in Fig. 1. Before the measurement, the coal was dried at 383 K in a vacuum oven for at least 12 h, and then 5 g of the sample was immediately placed into the adsorption cell and degassed for about 3 h. The measurements were conducted at pressures up to 5.0 MPa at 298 K.

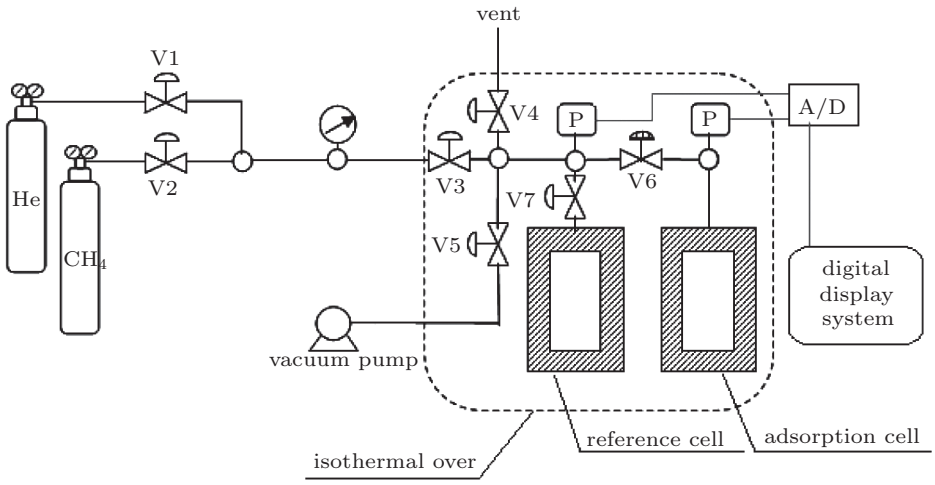


Fig. 1. Schematic arrangement of the experimental setup. V: needle valve, P: pressure transducer.

3. Results and discussion

3.1. Pore structure characteristics

The pore structure, including the surface area, pore volume, pore size distribution, and the surface morphology, is the key reservoir parameter, which directly affects the CBM production.[11] Based on the knowledge of the nature of coal and its pore system, N_2 adsorption/desorption, combined with SEM, could characterize the pore structure.[20]

In Table 3 the textural parameters for the coal samples are summarized. The pore size distributions are presented in Fig. 2. As shown in Table 3, the burial depth can change the coal texture, but neither the relationship between surface area and depth, nor the relationship between pore volume and depth is very noticeable. The sample Coal-1 has a larger surface area than others, and possesses the greatest pore volume within 1 to 10 nm size range. Sample Coal-2 has the lowest surface area and pore volume throughout the microporous range. The Coal-4, Coal-5, and Coal-6 have similar pore size distributions with a broad peak within a range of 2.5 nm to 10 nm. However, the pore size distributions of the Coal-1 and Coal-3, each of which possesses a great number of micropores, are very different from those of the other samples. The Coal-2, having a lower carbon content value of 63.42%, possesses a small number of micropores.

Table 3. Pore surface areas and pore volumes obtained by N_2 adsorption analyses of the coals.

Sample	Surface area, NLDFT/(m^2/g)	Pore volume, DFT /($\times 10^{-3}$ cm^3/g)
Coal-1	1.591	5.295
Coal-2	0.424	0.911
Coal-3	0.968	3.188
Coal-4	0.508	1.460
Coal-5	0.520	2.086
Coal-6	0.635	2.603

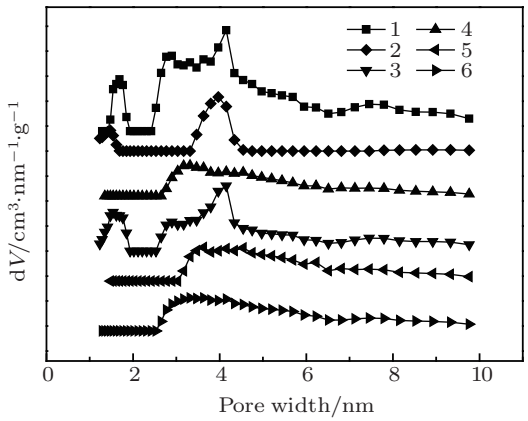


Fig. 2. Pore size distributions obtained by applying the DFT equation.

Figure 3 shows the SEM micrographs of coal samples. There is little difference in the surface morphology between samples Coal-2 and Coal-4, whose surfaces are smooth compared with those of the other samples. The surface morphologies of Coal-1, Coal-3, Coal-5, and Coal-6 look spongy compared with those of Coal-2 and Coal-4, indicating that the microporosity is well developed due to the large burial depth. The different burial depths result in different pore structures and degrees of graphitization.

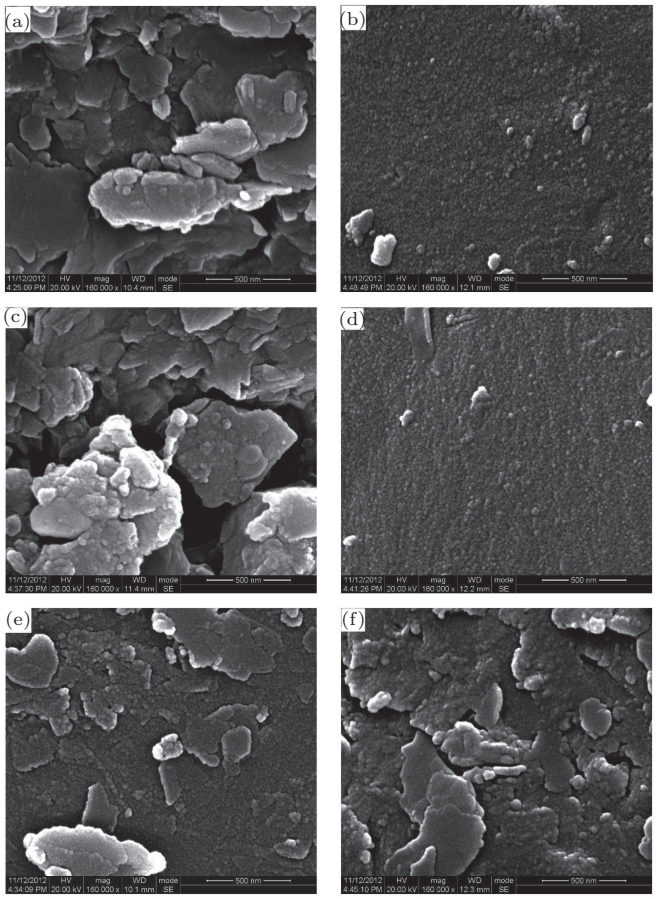


Fig. 3. SEM images of Coal-1 (a), Coal-2 (b), Coal-3 (c), Coal-4 (d), Coal-5 (e), and Coal-6 (f).

3.2. Proximate and ultimate analysis

The proximate and ultimate analyses of the coal samples are shown in Table 1 and Table 2, respectively. Each sample contains a certain quantity of volatiles. The proximate analysis results show that there is a difference between the samples. At the same location, the composition of coal is changed; and the content of volatile matter decreases as the burial depth increases, while the variation trend of fixed carbon content is reversed.

The ultimate analysis results show that at the same location, the increase in depth leads to the decreases in oxygen

content and the O/C ratio. The reduced amount of oxygen is involved in the formation of graphite-like structure. As illustrated in Fig. 4, the O/C ratio of the samples is negatively correlated to the burial depth. Different burial depths would result in large variations in temperature and gas pressure, which can promote the coalification process to some extent, and the number of oxygen groups decreases with the coal rank increasing. Thus, the increase in depth leads to the decreases in oxygen content and the O/C ratio within a range of burial depths.

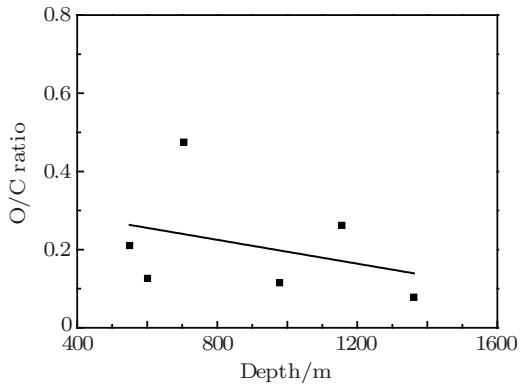


Fig. 4. O/C ratio versus burial depth.

3.3. Raman spectroscopy

The Raman spectra, characteristic of highly oriented carbon materials, provide averaged information about a large number of randomly distributed microcrystallites. Two bands appear in the first-order region (1000 cm^{-1}–2000 cm^{-1}): a prominent G band at $\sim$ 1580 cm^{-1}, attributed to a perfect graphite structure, and the D band (disordered) at $\sim$ 1350 cm^{-1}. The second-order region of the Raman spectra (2000 cm^{-1}–3000 cm^{-1}) presents a composite G' band that occurs at $\sim$ 2820 cm^{-1}.

Figure 5 shows the Raman spectra measured for the coal samples, and Table 4 presents positions and intensities of the Raman bands. It is clear that the G band is higher than the D band and at the same location, the relative intensity of D band decreases with burial depth increasing. Coal-3 has a better developed G band. The drop of the D band relative intensity indicates an improvement in the crystallite orientation of the sample. Therefore, graphite-like structures dominate over turbostratic structures in the samples.[24] The results in Table 4 confirm that the increase of depth slightly improves the structural order of the materials.

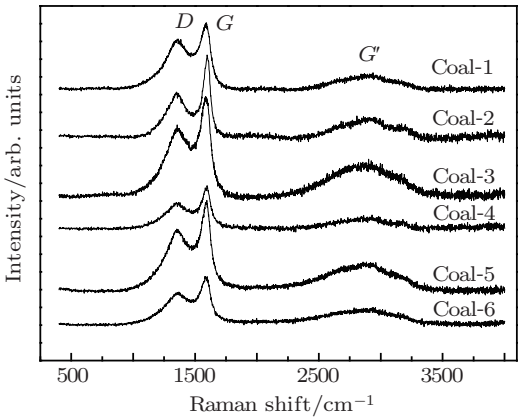


Fig. 5. Raman spectra for the coal samples.

Bands in the second-order region of the Raman spectrum are only observable in highly oriented carbon materials. Because of the heterogeneity of the samples studied, the particles that exhibit the G' band doublet should serve as an indication of the degree of crystallite order.[23] The relevant Raman parameter, I_D/I_G, which has already been mentioned to account for the degree of structural order, also confirms the significant improvement (I_D/I_G values of Coal-1, Coal-2, Coal-3, Coal-4, Coal-5, and Coal-6 are 0.753, 0.529, 0.677, 0.608, 0.676, and 0.670, respectively). The samples each undergo a solid-state type of graphitization in the stage of the coalification process. Basic structural units are arranged around the walls of pores, which flatten progressively as the depth increases. Thus, the evolutions of degree of graphitization and the crystallinity of these materials are mainly affected by the depth.

Table 4. Positions and intensities of the Raman bands measured for the studied materials.

Sample	D band		G band		G' band	
	P_D/cm^{-1}	I_D	P_G/cm^{-1}	I_G	$P_{G'}$/cm^{-1}	$I_{G'}$
Coal-1	1366.2	2101.3	1590.0	2791.1	2818.0	540.5
Coal-2	1360.0	1813.6	1598.0	3426.7	2824.4	709.7
Coal-3	1360.0	2821.6	1584.5	4166.3	2820.6	1378.1
Coal-4	1367.7	1094.3	1596.5	1799.3	2814.2	474.6
Coal-5	1358.5	2554.1	1595.0	3776.4	2821.8	1096.0
Coal-6	1357.0	1378.3	1580.0	2057.7	2820.6	650.2

3.4. FT–IR analysis

FT–IR spectra for samples are shown in Fig. 6. The samples exhibit similar FT–IR spectra, suggesting that they have similar structures and functional groups. A strong absorption band appears at around 3400 cm^{-1} that is assigned to –OH stretching. However, this peak is more pronounced in Coal-3, suggesting the presence of more –OH groups. The adsorption peaks are observed at 2900 cm^{-1}–3000 cm^{-1} and 1670 cm^{-1}–1760 cm^{-1} attributed to –COOH group vibrations. The peak appearing at 1000 cm^{-1}–1200 cm^{-1} can be attributed to esters, such as those in ethers, phenols, and hydroxyl groups. Shoulder bonds at low wavenumbers (830, 760, 670 cm^{-1}) may be related to out-of-plane bending modes. It is suggested that the changes in the intensities of the bands appearing between 1300 cm^{-1} and 900 cm^{-1} are due to oxygen surface groups and structure containing oxygen species mainly of a discrete nature.

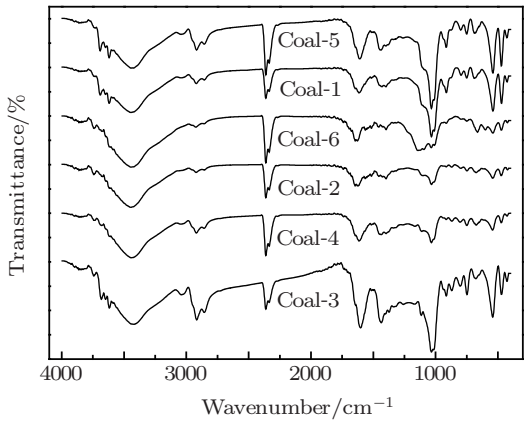


Fig. 6. FT–IR spectra of the studied samples.

The –OH radicals exist mainly in the terminal group and side chain; they are active and can be easily changed in the coalification process. In the coal, the –OH radicals exist in the polymeric structure, which would facilitate the formation of hydrogen bonds. As depth increases, both the aliphatic C–H stretching transmittance bands (3000 cm^{-1}–2920 cm^{-1}, 1450 cm^{-1}) and the hydrogen-bonded –OH transmittance band (3400 cm^{-1}) of the coal decrease and those of the aromatic ring increase.[26,27]

The 1600-cm^{-1} band is also observed to decrease as depth increases. Because this band is believed to be a polar substituent on the aromatic rings (such as –OH), the decrease, coupled with the decrease of the 3400-m^{-1} band (hydrogen-bonded –OH), suggests the disappearance of phenol –OH groups from aromatic structures in the coals.

3.5. CH_4 adsorption

The CH_4 adsorption data exhibit the isotherms of characteristic type-I behavior, classified by the International Union of Pure and Applied Chemistry (IUPAC). The Langmuir model is used to fit the data, and the fitting parameters are summarized in Table 5. The results show that Langmuir equation fits the experimental data well, and the coals in the Datong area have moderate adsorption capacities (Table 5), with Langmuir parameter, a, ranging from 0.352 mmol/g to 0.853 mmol/g. Here, a can be regarded as the maximum adsorption capacity, which represents the saturation adsorption capacity for methane adsorbed over the coal.

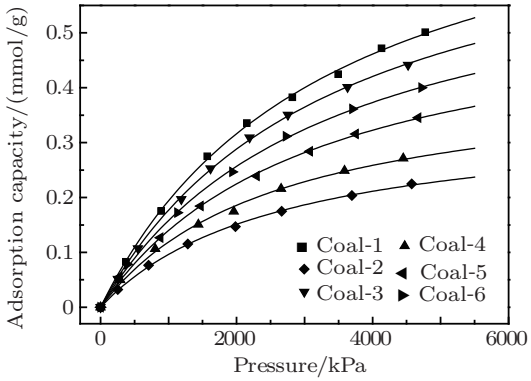


Fig. 7. CH_4 adsorption isotherms obtained by applying the Langmuir model at 298 K and the solid line for the data obtained from the Langmuir model.

Table 5. Langmuir parameters of equilibrium isotherms.

Sample	a/(mmol/g)	b/MPa^{-1}
Coal-1	0.853	0.295
Coal-2	0.352	0.378
Coal-3	0.777	0.294
Coal-4	0.425	0.388
Coal-5	0.571	0.324
Coal-6	0.683	0.301

Measurements of CH_4 adsorption capacity show that the adsorption capacity at low pressure substantially increases with the increasing of pressure and the subsequent plateau is due to saturation of adsorption capacity. The Coal-1 has the highest CH_4 adsorption capacity, while the sample Coal-2 possesses the lowest one.

The relationship between Langmuir maximum adsorption capacity, a and surface area is presented in Fig. 8(a). As a general trend, a is approximately proportional to the surface area of the samples. The positive relationship is observed between pore volume and a as shown in Fig. 8(b), which is consistent with the previous results.[11] In general, coals with the higher

surface area and pore volume, has a greater CH_4 adsorption capacity.[5,12] In Fig. 8(c), it appears that the O/C ratio does not exert a significant influence on the adsorption capacity of the coals, indicating that the O/C ratio is not a controlling factor for the CH_4 adsorption. This may be attributed to the difference in pore structure and composition among the samples. Figure 8(d) shows that the CH_4 adsorption capacity increases with the value of I_D/I_G increasing. Figure 8(e) shows that the maximum adsorption constant, α, first increases with depth increasing, then passes through a maximum and then decreases at greater depth.

Pore structure is the essential factor to affect CH_4 adsorption capacity of coal. However, other microstructural properties, including surface morphology, degree of graphitization, are all related to the stability of pore structure.

Variation in the burial depth can lead to the difference in microstructure, thus resulting in variation in CH_4 adsorption capacity. Adsorption capacity is an inherent feature of coal. Methane results from gas generation, migration, and accumulation processes, and is dependent on the burial history of the coal seams. Methane emission of coal seam increases with the increase of burial depth, and variation of pore structure of coals with depth illustrates the cause of this phenomenon.[28–32] Thus CH_4 adsorption capacity is determined by the burial depth to some extent.

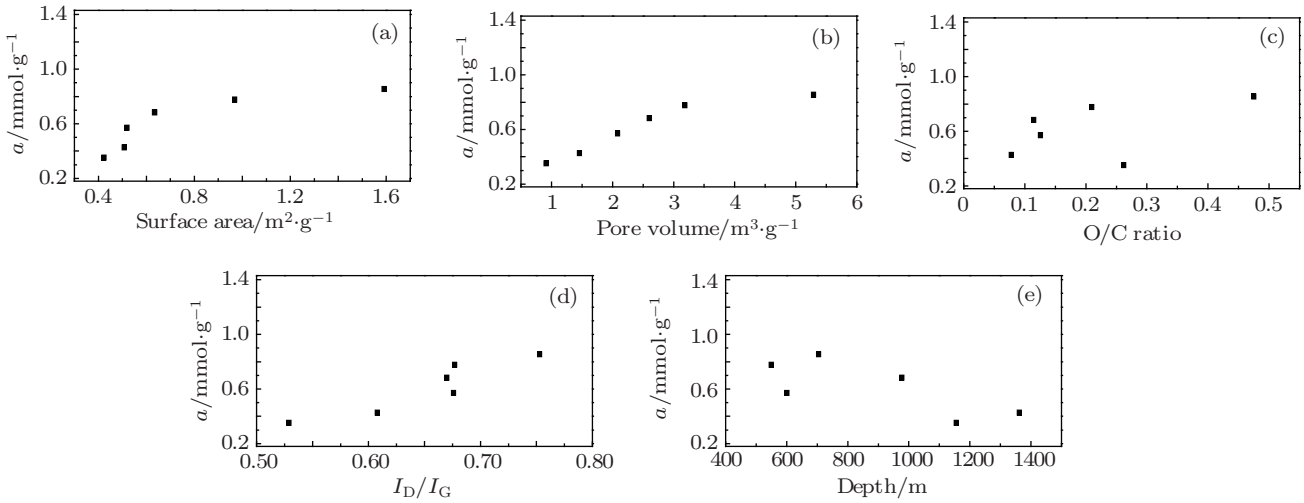


Fig. 8. Langmuir maximum adsorption capacity, a related to (a) surface area, (b) pore volume, (c) O/C ratio, (d) I_D/I_G, and (e) depth.

4. Conclusions

Variation in burial depth leads to the microstructural changes, including pore structure, degree of graphitization, and composition. The microstructural properties are used to analyze the variation in CH_4 adsorption capacity. The results show that Langmuir model fits well with the experimental data, and there are positive correlations among surface area, pore volume, I_D/I_G and CH_4 adsorption capacity. In addition, the burial depth can affect the CH_4 adsorption capacity of the coals, i.e., methane sorption capacity of coal seams can be calculated as a function of burial history.

Coal seams with high adsorption capacity can be characterized by the small content of methane migration. Since the permeability of coal is low, the outburst of methane would take place for the joint exploitation of coal and CBM, which will be dependent on further investigation on finding the balance between gas extraction and burial history.

References

[1] He M C and Zhao J 2013 *Chin. Phys. B* **22** 016802
[2] Li X C, Nie B S, Zhang R M and Chi L L 2012 *Int. J. Min. Sci. Technol.* **22** 885
[3] Nie B S, He X Q and Wang E Y 2000 *China Saf. Sci. J.* **10** 24
[4] Zhang T, Ellis G S, Ruppel S C, Milliken K and Yang R 2012 *Org. Geochem.* **47** 120
[5] Luo J J, Liu Y F, Jiang C F, Chu W, Jie W and Xie H P 2011 *J. Chem. Eng. Data* **56** 4919
[6] Yao Y, Liu D and Huang W 2011 *Int. J. Coal Geol.* **88** 135
[7] Moore T A 2012 *Int. J. Coal Geol.* **101** 36
[8] Zhang S, Yang S, Cheng J, Zhang B and Lu C 2011 *Procedia Engineering* **26** 327
[9] Wang Y L, Du B Y, Dou X M, Liu J, Shi B Y, Wang D S and Tang H X 2007 *Colloid Surface A* **307** 16
[10] Nie B S and Duan S M 1998 *Journal of Taiyuan University of Technology* **29** 417 (in Chinese)
[11] Hao S X, Wen J, Yu X P and Chu W 2013 *Appl. Surf. Sci.* **264** 433

[12] Liu D, Yao Y, Tang D, Tang S, Che Y and Huang W 2009 *Int. J. Coal Geol.* **79** 97
[13] Kedzior S and Jelonek I 2013 *Int. J. Coal Geol.* **111** 98
[14] Zhang D, Nie B S, Wang C, Zhao F, Guo J H, Liu X N, Li Q, Li H L and Zhang C 2011 *Procedia Engineering* **26** 1330
[15] Hu S, Li M, Xiang J, Sun L S, Li P S, Su S and Sun X X 2004 *Fuel* **83** 1307
[16] Kedzior S 2009 *Int. J. Coal Geol.* **80** 20
[17] Mastalerz M, Drobniak A, Strapoc D, Solano A W and Rupp J 2008 *Int. J. Coal Geol.* **76** 205
[18] Cai Y, Liu D, Yao Y, Li J and Qiu Y 2011 *Int. J. Coal Geol.* **88** 101
[19] Zhang S H, Tang S H, Tang D Z, Pan Z J and Yang J 2010 *Int. J. Coal Geol.* **81** 117
[20] Wang Y, Du B, Dou X, Liu J, Shi B, Wang D and Tang H 2007 *Colloid Surface A* **307** 16
[21] Wang S F, Yan G Y, Chen S S, Bai Z L, Wang J L, Yu W and Fu G S 2013 *Chin. Phys. B* **22** 037302
[22] Zhao X W, Gao X Y, Chen X M, Chen C and Zhao M K 2013 *Chin. Phys. B* **22** 024202
[23] Smedowski L, Krzesinska M, Kwasny W and Kozanecki M 2011 *Energ. Fuel* **25** 3142
[24] Li C Y, Zhao J T, Fang Y T and Wang Y 2009 *Energ. Fuel* **23** 5099
[25] Mastalerz M, Drobniak A, Walker R and Morse D 2010 *Int. J. Coal Geol.* **83** 467
[26] Landais P and Gerard L 1996 *Int. J. Coal Geol.* **30** 285
[27] Goodman A L, Campus L A and Schroeder K T 2005 *Energ. Fuel* **19** 471
[28] Liu F S, Chu W, Sun W J, Xue Y and Jiang Q 2012 *J. Nat. Gas Chem.* **21** 708
[29] Jiang Q, Chu W, Sun W J, Liu F S and Xue Y 2012 *Acta Phys. Chim. Sin.* **28** 1101
[30] Wang J, Dong B Z, Xu Y, Li Z H, Fan W H, Wu D and Sun Y H 2003 *Acta Phys. Sin.* **52** 635 (in Chinese)
[31] Liang J Q, Liang Z Z, Zhu W B and Su F G 2011 *Acta Phys. Sin.* **60** 057802 (in Chinese)
[32] Ma X X, Guo G W, Tang G Z, Sun M R and Wang L Q 2013 *Chin. Phys. B* **22** 056202